Proc. of the XI Int. Conf. — Ion Implantation and other Applications of Ions and Electrons, Kazimierz Dolny 2016

Production of Molybdenum and Tantalum Ion Beams using CCl_2F_2

M. Turek[a,*], A. Drożdziel[a], K. Pyszniak[a], J. Filiks[a], S. Prucnal[a], D. Mączka[a], Yu. Vaganov[b] and P. Węgierek[c]

[a]Institute of Physics, Maria Curie-Skłodowska University, Pl. M. Curie-Skłodowskiej 1, 20-031 Lublin, Poland
[b]Laboratory of Nuclear Problems, JINR Dubna, Russia
[c]Lublin University of Technology, Nadbystrzycka 38A, 20-618 Lublin, Poland

A new method of refractory metal (like Mo and Ta) ion beam production using the arc discharge ion source and CCl_2F_2 (dichlorodifluoromethane) used as a feeding gas supported into the discharge chamber is presented. It is based on etching of the refractory metal parts (e.g. anode or a dedicated tube) Cl and F containing plasma. The results of measurements of the dependences of ion currents on the working parameters like discharge and filament currents as well as on the magnetic field flux density of an external electromagnet coil are shown and discussed. The separated Mo^+ and Ta^+ beam currents of approximately 22 μA and 2 μA, respectively, were obtained.

DOI: 10.12693/APhysPolA.132.283
PACS/topics: 07.77.Ka, 34.80.Dp, 61.72.uj

1. Introduction

Ion implantation has become one of the most popular methods of modification of physicochemical, optical and mechanical properties of a wide spectrum of materials including semiconductors [1, 2], metals [3, 4] and polymers [5, 6] as well as quantum dots [7]. In order to cope with the demands of providing intense, high quality beams of a variety of ions numerous designs of ion sources and ion beam production procedures were invented [8, 9].

The refractory metals, like Mo or Ta, implantations are applied in order to improve corrosion resistance of such metals as aluminum and steel [10, 11] or magnesium alloys [12]. Passive layers on the surface of stainless steel formed by Mo implantation that resulted in improvement of its resistance on corrosion [13], also Ta implantation to the Al–Mg alloys increased the oxidation resistance of that alloy [14] as well as hardness and elastic modulus of the Mo implanted aluminum alloy [15]. A similar effect of increased hardness and reduced friction coefficient was observed in the case of the Ta implanted Al–Mg alloy as a result of Ta_2O_5 layer formation [16]. The effect of low-energy Ta implantation on hardness and other mechanical properties of irradiated sapphire was studied [17]. Production of solid lubricant MoS_2 layers in Al_2O_3, ZrO_2 and SiO_2 oxides by Mo and S implantations was also under investigation [18].

The most popular method for refractory metal ion beam production is using the metal vapor vacuum arc (MEVVA) ion sources [19, 20]. Another effective method is applying volatile compounds as a feeding gas to the electron cyclotron ion source [21]. The other methods to be mentioned are: plasma sputtering [22], laser ablation combined with electron cyclotron resonance [23], electron beam ionisation [24] especially in the version with the high power evaporator/target heating systems [25].

The production of intense Mo^+ ion beam as a result of chemical sputtering of anode by the chlorine containg plasma was already reported as a "side effect" of rare earths ions production from their chlorides [26]. The method based on the arc discharge ion source [27, 28] was developed later using chlorine derivatives of methane, like CCl_4 and $CHCl_3$ as feeding gases [29]. Mo^+ ion beams (currents ≈ 18 μA) were obtained. However, the method failed to produce Ta ion beams of satisfactory intensity. Dichlorodifluoromethane CCl_2F_2 (also known as Freon-12, R12, used over years as a refrigerant and aerosol spray propellant) is known to enhance sputtering yields of metals [30]. It is also known that F containing plasma is a good etchant of Mo, Ta, and other refractory metals [31]. Therefore, we decided to test CCl_2F_2 as a feeding gas in the arc discharge ion source.

The paper contains brief description of the arc discharge ion source and the experimental setup. Basic characteristics of the ion source are presented and discussed in the paper in order to find optimal working conditions for effective ion beam production. These include dependences of extracted ion current and discharge voltage on the discharge and filament currents as well as on the magnetic field flux density due to the external electromagnet. Changes of ion yield and discharge voltage due to the CCl_2F_2 flow are also under investigation in order to confirm the important role of Cl and F containing plasma etching in effective ion production. The presented measurements were made for molybdenum and tantalum.

2. Experimental

The ion source used for refractory metals ion beam production was the arc discharge ion source witch cylindrical anode presented in [26–29]. In the considered case

*corresponding author; e-mail: mturek@kft.umcs.lublin.pl

the ion source was configured without any internal evaporator. The schematic view of the ion source is shown in Fig. 1. The basic parts of the ion source as the anode and cathode filament mounts are made of molybdenum, although any other refractory metal could be used. For Ta ions production a tube made of the 1 mm thick tantalum sheet was placed inside the anode. Its external diameter was equal to the internal diameter of the anode. A long stainless steel capillary was used to provide the feeding gas to the inlet. The ionisation chamber was formed by anode and filament mounts of the internal diameter of $\approx 10-11$ mm and the length of ≈ 20 mm. A spiral filament made of tungsten wire (diameter of 0.75) was placed along the chamber axis. The cathode filament is heated by the high current I_c (up to ≈ 38 A). The hot wire was the source of primary electrons maintaining the arc discharge between the anode and the cathode. The stabilized discharge current I_a is usually set up to 4 A while the discharge voltage is typically in the range 25–40 V. In order to initialize the discharge, the anode voltage is set at ≈ 100 V and the electron emission is increased by rising I_c, the discharge voltage stabilizes at lower values after 10–15 min after the ignition. The discharge chamber is surrounded by the electromagnet coil. The additional external magnetic field of axial symmetry in the discharge chamber region is used to compensate the magnetic field from the spiral cathode. It also helps to shift the discharge region near the extraction hole.

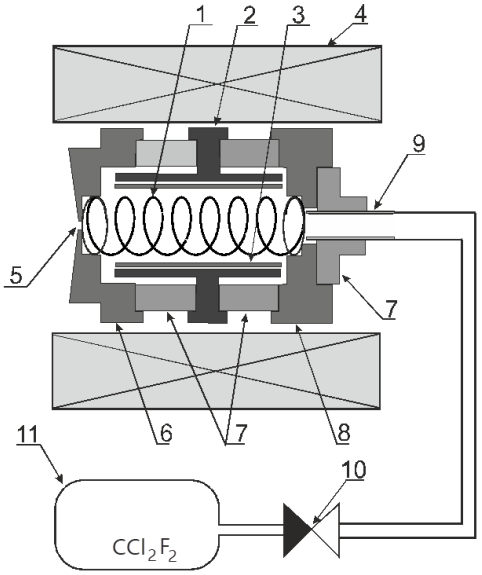

Fig. 1. Schematic view of the ion source. 1- cathode filament, 2 -anode, 3 - optional tubular insert, 4 - electromagnet, 5 - extraction hole, 6 and 8 - cathode mounts, 7 - insulators, 9- gas inlet, 10 - dosing valve, 11 - container with freon gas.

The gaseous CCl_2F_2 is transported through the dosing valve into the discharge chamber via the capillary gas inlet. It is known that R12 and other freon molecules decompose in hot plasma, hence the plasma inside the chamber is enriched by Cl and F ions, atoms and molecules to a large extent [32, 33]. The presence of residual water may also result in production of fluoric and chloric acids [34]:

$$CCl_2F_2 + 2H_2O \rightarrow 2HCl + 2HF + CO_2. \quad (1)$$

Both fluorine and chlorine containing plasma is a very good etchant of metallic molybdenum, especially at elevated temperatures [35–37]. The rates of tantalum etching rates can reach also the values of several μm per minute [38, 39]. Different Mo or Ta halide molecules are released to plasma [36] and then destroyed and ionised by electron impact in the discharge region, however, small amounts of molecular halide ions are observed after mass-separation. The produced ions are extracted through the extraction opening of the diameter $\approx 0.8-1$ mm using the extraction voltage $V_{ext} = 25$ kV. The extracted beam is formed using a triplet lens system and the beam enters a 90° sector separating electromagnet. The mass-separated beamlet is accelerated using the additional voltage $V_{acc} = 75$ keV. The ion currents of beamlets are measured making use of a Faraday cup placed behind the acceleration tube.

3. Results

Characteristics of the ion source were determined $\approx$ 30 min after the discharge was initialized when the ions source worked stable. Basic working characteristics were measured including dependences of ion current and discharge voltage on the discharge voltage I_a, filament current I_c as well as on the magnetic field flux density B. Figure 2 presents the dependences of the mass-separated Mo^+ and Ta^+ currents on the discharge current I_a. The other working parameters (i.e. filament current I_c, magnetic field flux density B and the feeding gas flow Φ) were constant. The increase of I_{ion} with I_a was observed and the I_{ion} (I_a) curve reached its maximum at $I_a = 2$ A (Mo) or $I_a = 3$ A (Ta). The ion current decreased for larger I_a. This effect was better visible in the case of Mo, a large degradation of the ion current for larger I_a could be seen.

There are several reasons for the saturation of $I_{ion}(I_a)$ curves. One of them is the fact that as the plasma density rises the extraction efficiency decreases due to screening properties of plasma. It should be also noted that the discharge voltage U_a rises with the discharge current. This was observed for the previously reported Mo ions production method [29] and the low melting point and volatile feeding substances [27]. The most important factor could be, however, the change of ionisation efficiency with the discharge voltage, and, consequently with the mean energy of electrons in the discharge.

One can see in Fig. 2 that the the discharge voltage in the range 30–50 V seems to be optimal for Mo^+ production. In the case of Ta^+ ions the optimal discharge voltage is slightly lower, in the range 30–40 V. It is even better visible in Fig. 3 presenting $I_{ion}(I_c)$ and $U_a(I_c)$ characteristics. One deals here with the two concurrent tendencies. Firstly, the larger is the filament current, the

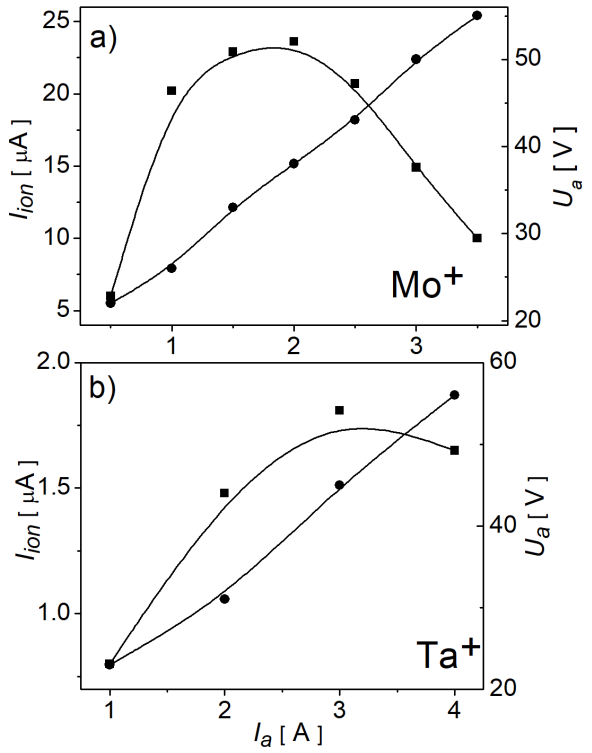

Fig. 2. Ion current (squares) and discharge voltage (circles) as functions of discharge current.

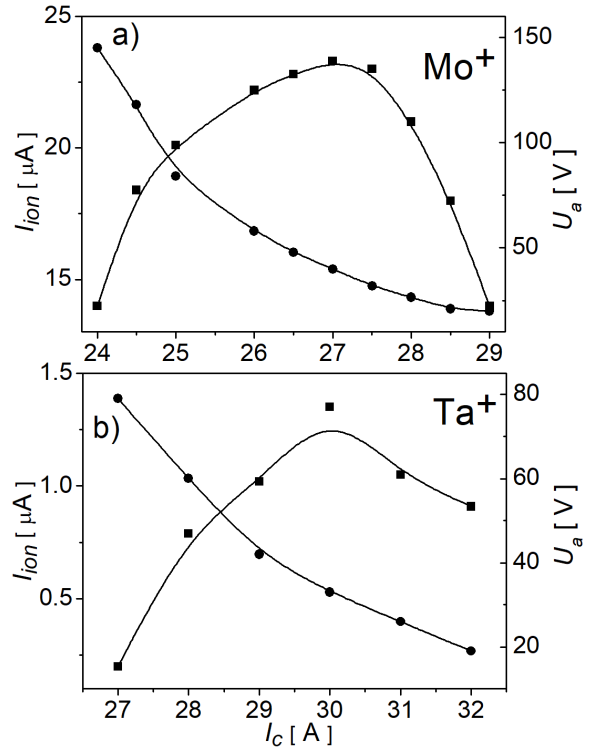

Fig. 3. Ion current (squares) and discharge voltage (circles) as functions of filament current.

more electrons are emitted from the hotter filament and, hence, the ionization probability increases. On the other hand, higher electron density leads to the drop of U_a and, therefore, to the decrease of mean electron energy. Hence, ionization efficiency decreases when U_a is too low. This, in connection with the fact that electron impact ionisation cross-section of both considered elements has a maximum for several tens of volts, could explain both the saturation of $I_{ion}(I_a)$ curves and the presence of the maximum in $I_{ion}(I_c)$.

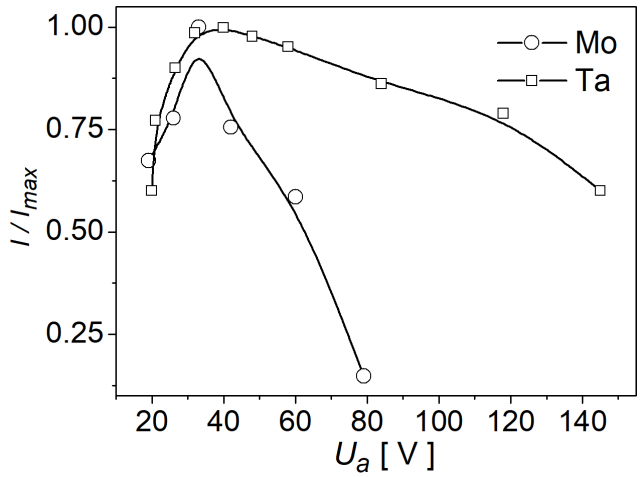

Fig. 4. Normalized ion currents as functions of discharge voltage.

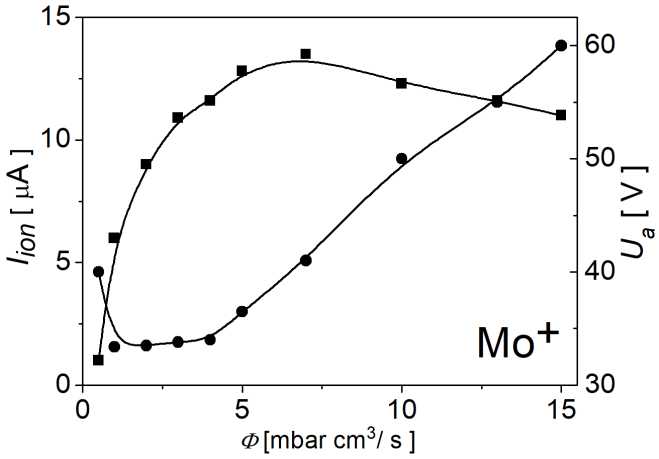

Fig. 5. Ion current (squares) and discharge voltage (circles) as functions of CCl_2F_2 feeding gas flow.

The $I_{ion}(I_c)$ and $U_a(I_c)$ curves transformed to the normalised I_{ion} dependence on the discharge voltage are presented in Fig. 4. One could see that the overall trend of these curves resemble that of the electron impact ionisation cross-section on the electron energy.

Ion yield strongly depends on the feeding gas flow. This is confirmed by the data shown in Fig. 5. The ion

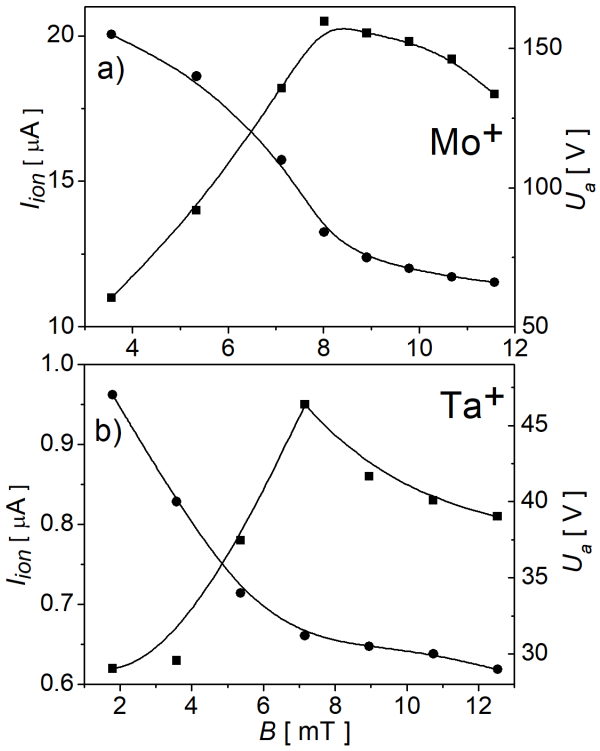

Fig. 6. Ion current (squares) and discharge voltage (circles) as functions of external electromagnet magnetic field flux density.

current increases very fast ion production is supressed right after the dosing valve is closed. One should be aware of the fact that high CCl_2F_2 leak makes vacuum conditions poorer which in turn makes the ion beam transport less effective and can lead to electrical breakdowns between the extraction electrode and the ion source. The optimal flow is ≈ 7 mbar cm^{3}s^{-1}. Further increase of Φ leads to excessive rise of the discharge voltage.

The dependencies of ion current and discharge voltage on the magnetic flux density produced by the external electromagnet coil were measured in order to investigate the influence of magnetic field on the ion source effciency. The results are shown in Figure 6.

The magnetic flux density was measured using the LakeShore model 450 gaussmeter. For both Mo and Ta the maximal ion current was registered for the B values about 7 mT. Such B value is more or less needed to compensate the field from the spiral filament. Moreover, the external field helps to form the discharge plasma region in order to make the extraction as effective as possible. It should be noted that increasing the magnetic feld flux could lead to the reducion of discharge voltage and degrade ionisation efficiency.

4. Conclusions

A new method of refractory metal ion beams like Mo or Ta using the plasma ion source and dichlorodifluoromethane as a working gas is presented in the paper. It is based on the fact that plasma containing Cl and F etches the mentioned metals relatively fast. Basic working characteristics of the ion source are presented and discussed in the paper including dependences of the ion current on the anode and filament currents as well as on the external magnetic field flux density. It was found that the optimal discharge voltage is in the range 30-50 V for both considered metals, and the optimal magnetic field flux density is ≈ 7 mT. CCl_2F_2 flow should be kept no larger than ≈ 7 mbar cm^{3}s^{-1}, as the larger flow makes vacuum condition poor and also decreases the discharge voltage. The reduction of discharge voltage and the ion yield is also observed for the discharge currents larger than 2–2.5 A. One may expect that other chlorine and fluorine derivatives of hydrocarbons as well as substances like sulfur hexafluoride can be also successfully applied using the described method.

References

[1] F. Komarov, L. Vlasukova, O. Milchanin, A. Mudryi, B. Dunets, W. Wesch, E. Wendler, *Phys. Status Solidi A* **209**, 148 (2012).

[2] S. Prucnal, S.-Q. Zhou, X. Ou, H. Reuther, M.O. Liedke, A. Mücklich, M. Helm, J. Zuk, M. Turek, K. Pyszniak, W. Skorupa, *Nanotechnology* **23**, 485204 (2012).

[3] J. Bowsher, A. Hussain, P. Williams, J. Nevelos, J.C. Shelton, *J. Arthropl.* **19**, 107 (2004).

[4] P. Budzynski, J. Sielanko, *Acta Phys. Pol. A* **128**, 841 (2015).

[5] A.M. Abdul-Kader, A. Turos, D. Grambole, J. Jagielski, A. Piatkowska, N.K. Madi, M. Al-Maadeed, *Nucl. Instrum. Methods Phys. Res. B* **240**, 152 (2005).

[6] V.N. Popok, *Rev. Adv. Mater. Sci.* **30**, 1 (2012).

[7] S. Prucnal, M. Glaser, A. Lugstein, E. Bertagnolli, M. Stoegger-Pollach, S. Zhou, M. Helm, D. Reichel, L. Rebohle, M. Turek, J. Żuk, W. Skorupa, *Nano Res.* **7**, 179 (2014).

[8] I.G. Brown, *The Physics and Technology of Ion Sources*, Wiley, Weinheim 2004.

[9] H. Zhang, *Ion Sources*, Sci. Press, Beijing, and Springer, Berlin 1999.

[10] C.M. Abreu, M.J. Cristóbal, R. Figueroa, G. Pena, *Corros. Sci.* **54**, 143 (2012).

[11] W. Zhongda, L. Songmei, *Acta Phys.-Chim. Sin.* **8**, 401 (1992).

[12] X. Wang, X. Zeng, G. Wu, S. Yao, Y. Lai, *J. Alloys Comp.* **437**, 87 (2007).

[13] C.M. Abreu, M.J. Cristóbal, R. Figueroa, X.R. Novoa, G. Pena, M.C. Perez, *Def. Diff. Forum* **289–292**, 175 (2009).

[14] X. Wang, X. Zeng, G. Wu, S. Yao, L. Li, *Nuclear Instrum. Methods Phys. Res. B* **263**, 401 (2007).

[15] R. Figueroa, C.M. Abreu, M.J. Cristóbal, G. Pena, *Wear* **276-277**, 53 (2012).

[16] D.Y. Zhang, Q.Y. Fei, H.M. Zhao, M. Geng, X.C. Zeng, P.K. Chu, *Thin Solid Films* **484**, 215 (2005).

[17] W. Ensinger, R. Nowak, *Nucl. Instrum. Methods* **80**, 1085 (1993).

[18] A.K. Rai, R.S. Bhattacharya, S.C. Kung, *J. Appl. Phys.* **68**, 5169 (1990).

[19] I.G. Brown, B. Feinberg, J.E. Galvin, *J. Appl. Phys.* **63**, 4889 (1988).

[20] B.X. Liu, D.H. Zhu, H.B. Lu, K. Tao, *MRS Proc.* **316**, 795 (1993).

[21] H. Koivisto, J. Arje, M. Nurmia, *Rev. Sci. Instrum.* **69**, 785 (1998).

[22] M. Kanter, *Nucl. Instrum. Methods Phys. Res. B* **70**, 200 (1992).

[23] S. Gammino, L. Torrisi, G. Ciavola, L. Ando, J. Wolowski, L. Laska, J. Krasa, A. Picciotto, *Nucl. Instrum. Methods Phys. Res. B* **209**, 345 (2003).

[24] J. M. Nitschke, *Nucl. Instrum. Methods Phys. Res. A* **236**, 1 (1985).

[25] Y.V. Yushkevich, M. Turek, D. Mączka, K. Pyszniak, B. Słowiński, Y.A. Vaganov, *Nukleonika* **57**, 351 (2012).

[26] M. Turek, S. Prucnal, A. Droździel, K. Pyszniak, *Rev. Sci. Instrum.* **80**, 043304 (2009).

[27] M. Turek, A. Droździel, K. Pyszniak, S. Prucnal, *Nucl. Instrum. Methods Phys. Res. B* **269**, 700 (2011).

[28] M. Turek, A. Drozdziel, K. Pyszniak, S. Prucnal, J. Zuk, *Przeglad Elektrotechniczny* **86**, 193 (2010) (in Polish).

[29] M. Turek, A. Droździel, K. Pyszniak, S. Prucnal, D. Mączka, *Acta Phys. Pol. A* **125**, 1388 (2014).

[30] J. Sielanko, J. Filiks, M. Sowa, J. Zinkiewicz, M. Drewniak, *Vacuum* **46**, 1459 (1995).

[31] *Functionalized Inorganic Fluorides: Synthesis, Characterization and Properties of Nanostructured Solids*, Ed. A. Tressaud, Wiley 2010.

[32] Y. Wang, W. Lee, C. Chen, L. Hsieh, *Environ. Sci. Technol.* **33**, 2234 (1999).

[33] J. Radic-Peric, A. Dasic, *J. Therm. Anal. Calorim.* **79**, 59 (2005).

[34] M. Ohno, Y. Ozawa, T. Ono, *Int. J. Plasma Environm. Sci. Technol.* **1**, 159 (2007).

[35] V.M. Donnelly, A. Kornblit, *J. Vac. Sci. Technol. A* **31**, 050825 (2013).

[36] A.I. Picard, G. Turban, *Plasma Chem. Plasma Proces.* **5**, 333 (1985).

[37] D.S. Fischl, D.W. Hess, *J. Vac. Sci. Technol. B* **6**, 1577 (1988).

[38] V.J. Tu, J.Y. Jeong, A. Schutze, S.E. Babayan, G. Ding, S. Selwyn, R.F. Hicks, *J. Vac. Sci. Technol. A* **18**, 2799 (2000).

[39] M. Yamada, M. Nakaishi, K. Sugishima, *J. Electrochem. Soc.* **138**, 496 (1991).